

# Study of the electromagnetic transition form-factors in $\eta \rightarrow \mu^+ \mu^- \gamma$ and $\omega \rightarrow \mu^+ \mu^- \pi^0$ decays with NA60

R. Arnaldi<sup>a</sup>, K. Banicz<sup>b,c</sup>, J. Castor<sup>d</sup>, B. Chaurand<sup>e</sup>, C. Cicalò<sup>f</sup>, A. Colla<sup>a</sup>, P. Cortese<sup>a</sup>, S. Damjanovic<sup>b,c,1</sup>, A. David<sup>b,g</sup>, A. de Falco<sup>f</sup>, A. Devaux<sup>d</sup>, L. Ducroux<sup>h</sup>, H. En'yo<sup>i</sup>, J. Fargeix<sup>d</sup>, A. Ferretti<sup>a</sup>, M. Floris<sup>f</sup>, A. Förster<sup>b</sup>, P. Force<sup>d</sup>, N. Guettet<sup>b,d</sup>, A. Guichard<sup>h</sup>, H. Gulkanian<sup>j</sup>, J. M. Heuser<sup>i</sup>, M. Keil<sup>b,g</sup>, L. Kluberg<sup>e</sup>, J. Lozano<sup>g</sup>, F. Manso<sup>d</sup>, P. Martins<sup>b,g</sup>, A. Masoni<sup>f</sup>, A. Neves<sup>b</sup>, H. Ohnishi<sup>i</sup>, C. Oppedisano<sup>a</sup>, P. Parracho<sup>b,g</sup>, P. Pillot<sup>h</sup>, T. Poghosyan<sup>j</sup>, G. Puddu<sup>f</sup>, E. Radermacher<sup>b</sup>, P. Ramalhete<sup>b,g</sup>, P. Rosinsky<sup>b</sup>, E. Scomparin<sup>a</sup>, J. Seixas<sup>g</sup>, S. Serçi<sup>f</sup>, R. Shahoyan<sup>b,g</sup>, P. Sonderegger<sup>g</sup>, H. J. Specht<sup>c,1</sup>, R. Tieulent<sup>h</sup>, G. Usai<sup>f</sup>, R. Veenhof<sup>b</sup>, H. K. Wöhri<sup>f,g</sup>,  
(NA60 Collaboration)

<sup>a</sup>Università di Torino and INFN, Italy

<sup>b</sup>CERN, Geneva, Switzerland

<sup>c</sup>Physikalisches Institut der Universität Heidelberg, Germany

<sup>d</sup>LPC, Université Blaise Pascal and CNRS-IN2P3, Clermont-Ferrand, France

<sup>e</sup>LLR, Ecole Polytechnique and CNRS-IN2P3, Palaiseau, France

<sup>f</sup>Università di Cagliari and INFN, Cagliari, Italy

<sup>g</sup>IST-CFTP, Lisbon, Portugal

<sup>h</sup>IPN-Lyon, Univ. Claude Bernard Lyon-1 and CNRS-IN2P3, Lyon, France

<sup>i</sup>RIKEN, Wako, Saitama, Japan

<sup>j</sup>YerPhI, Yerevan, Armenia

## Abstract

The NA60 experiment at the CERN SPS has studied low-mass muon pairs in 158A GeV In-In collisions. The mass and  $p_T$  spectra associated with peripheral collisions can quantitatively be described by the known neutral meson decays. The high data quality has allowed to remeasure the electromagnetic transition form factors of the Dalitz decays  $\eta \rightarrow \mu^+ \mu^- \gamma$  and  $\omega \rightarrow \mu^+ \mu^- \pi^0$ . Using the usual pole approximation  $F = (1 - M^2/\Lambda^2)^{-1}$  for the form factors, we find  $\Lambda^{-2}$  (in  $\text{GeV}^{-2}$ ) to be  $1.95 \pm 0.17(\text{stat.}) \pm 0.05(\text{syst.})$  for the  $\eta$  and  $2.24 \pm 0.06(\text{stat.}) \pm 0.02(\text{syst.})$  for the  $\omega$ . While the values agree with previous results from the Lepton-G experiment, the errors are greatly improved, confirming now on the level of  $10\sigma$  the strong enhancement of the  $\omega$  form factor beyond the expectation from vector meson dominance. An improved value of the branching ratio  $\text{BR}(\omega \rightarrow \mu^+ \mu^- \pi^0) = [1.73 \pm 0.25(\text{stat.}) \pm 0.14(\text{syst.})] \cdot 10^{-4}$  has been obtained as a byproduct.

*Key words:* Lepton Pairs, Transition form factor, Conversion decays

*PACS:* 13.85.Qk, 13.40.Gp, 13.20.-v

## 1. Introduction

The standard electromagnetic decay modes of light unflavored mesons ( $S=C=B=0$ ) include the so-called Dalitz decays  $A \rightarrow B l^+ l^-$ . Here, the meson  $A$  decays into an object  $B$  (a photon or another meson) and a lepton pair, formed by internal conversion of an intermediate virtual photon with invariant mass  $M$ . Assuming point-like particles, the decay rate of this process

vs.  $M$  can exactly be described by QED [1]. However, the rate is strongly modified by the dynamic electromagnetic structure arising at the vertex of the transition  $A \rightarrow B$ . This modification is formally described by a (multiplicative) *transition form factor*  $|F_{AB}(M)|^2$ . A major element governing  $|F_{AB}|^2$  is the resonance interaction between photons and hadrons in the time-like region, commonly referred to as vector meson dominance (VMD). Experimentally,  $|F_{AB}(M)|^2$  is directly accessible by comparing the measured invariant mass spectrum of the lepton pairs from Dalitz decays with the point-like QED prediction. A comprehensive review of the topic

<sup>1</sup>Corresponding authors sdamjano@cern.ch (S. Damjanovic), specht@physi.uni-heidelberg.de (H. J. Specht)

is contained in [2].

The physics interest in studying Dalitz decays and the associated transition form factors is twofold. First, the electromagnetic interaction continues to be an extremely useful tool to gain deeper insight into meson structure, while the role of the resonance interaction in this context is far from being quantitatively settled. Because the experiments are very difficult, the quality of the existing data is generally poor. Second, and related to the last point, the study of *direct* production of dileptons in high-energy nuclear collisions in the context of thermal radiation requires a precise and complete knowledge of the characteristics and the relative weights for the existing decay channels, and this is universally true at all facilities where such studies are ongoing (SIS, SPS, RHIC, and FAIR in the future). Disregarding the case of the  $\pi^0$ , the major two Dalitz decays contributing to the mass range  $M > 0.2$  GeV are those of the  $\eta$ (548) and the  $\omega$ (782). For the dielectron channel, the existing results on  $|F|^2$  for the  $\eta$  [3] and  $\omega$  [4] are not accurate enough for meaningful physics conclusions. For the dimuon channel, however, significant results on  $|F|^2$  have been obtained by the Lepton-G experiment, both for  $\eta \rightarrow \mu^+\mu^-\gamma$  [5] and for  $\omega \rightarrow \mu^+\mu^-\pi^0$  [6]. Using the usual pole approximation [2]

$$|F|^2 = (1 - M^2/\Lambda^2)^{-2} \quad (1)$$

for the form factors,  $\Lambda^{-2}$  has been found to be  $1.9 \pm 0.4$  GeV $^{-2}$  for the  $\eta$  and  $2.36 \pm 0.21$  GeV $^{-2}$  for the  $\omega$ . While the value for the  $\eta$  is compatible with VMD within its large error, the value for the  $\omega$  exceeds that expected from VMD ( $1.69$  GeV $^{-2}$ ) by 3 standard deviations. This discrepancy, statistically significant, has remained unexplained up to today. Numerically, the associated enhancement of the mass-differential decay rate relative to that for VMD amounts to about one order of magnitude at  $M = 0.6$  GeV, i.e. close to the kinematic limit of  $M_\omega - M_{\pi^0} = 0.648$  GeV, with corresponding consequences for values and systematic errors of the yield of excess dileptons observed in this mass region [7, 8, 9, 10, 11].

In this Letter, we present new results on the transition form factors of the Dalitz decays  $\eta \rightarrow \mu^+\mu^-\gamma$  and  $\omega \rightarrow \mu^+\mu^-\pi^0$ . They have been obtained as a byproduct of the ongoing analysis of low-mass dimuon production in 158A GeV In-In collisions, exploiting here the nearly  $pp$ -like peripheral rather than the more central interactions associated with excess dileptons [8, 9, 10]. The high data quality has enabled us to greatly improve the accuracy of the form factor measurements as compared to the Lepton-G experiment.

## 2. Experiment

The NA60 experiment at the CERN SPS is described in detail in [12]. In short, the apparatus complements the muon spectrometer previously used by NA50 with a high-granularity radiation-hard silicon pixel telescope, placed inside a 2.5 T dipole magnet. The telescope tracks all charged particles upstream of the hadron absorber and determines their momenta independently of the muon spectrometer. The matching of the muon tracks before and after the absorber, both in *coordinate and momentum space*, strongly improves the dimuon mass resolution in the low-mass region and reduces the combinatorial background due to  $\pi$  and  $K$  decays. The additional bend by the dipole field greatly improves the opposite-sign dimuon acceptance at low masses and low transverse momenta. The rapidity coverage is  $0.3 < y_{cm} < 1.3$  in this region. The selective dimuon trigger and the radiation-hard vertex tracker with its high read-out speed allow the experiment to run at very high rates for extended periods, leading to an unprecedented level of statistics for low-mass lepton pairs.

## 3. Analysis Procedure

The results reported in this Letter were obtained from the analysis of data taken in 2003 for 158A GeV In-In collisions. The analysis procedure is also described in detail in [12]. The essential steps of the data reconstruction concern the tracking in the two spectrometers, vertex finding, and matching of the tracks. Matching is done by selecting those associations between the muon- and pixel-spectrometer tracks which give the smallest weighted squared distance (*matching*  $\chi^2$ ) between the two tracks, in the space of angles and inverse momenta, taking into account their error matrix [12]. The combinatorial background of uncorrelated muon pairs originating from  $\pi$  and  $K$  decays is determined by a *mixed-event technique*. After subtraction of the combinatorial background, the remaining opposite-sign pairs still contain “signal” fake matches (associations of genuine muons to non-muon vertex tracks). These have a shape of the matching  $\chi^2$  distributions different from those of the true matches. They are determined either by an overlay Monte Carlo method (used here) or by event mixing [12], with identical results, and are then also statistically subtracted from the data. The collision centrality of the events is defined through the total charged-particle rapidity density as measured by the silicon pixel telescope.

For the purpose of this Letter, solely peripheral In-In collisions are considered. To keep sufficient events,

they are selected through the cut in multiplicity density  $4 < dN_{ch}/d\eta < 30$ , with an average multiplicity density  $\langle dN_{ch}/d\eta \rangle = 17$ . The raw opposite-sign, background and signal dimuon mass spectra for this peripheral selection are shown in Fig. 1. After subtracting the relatively

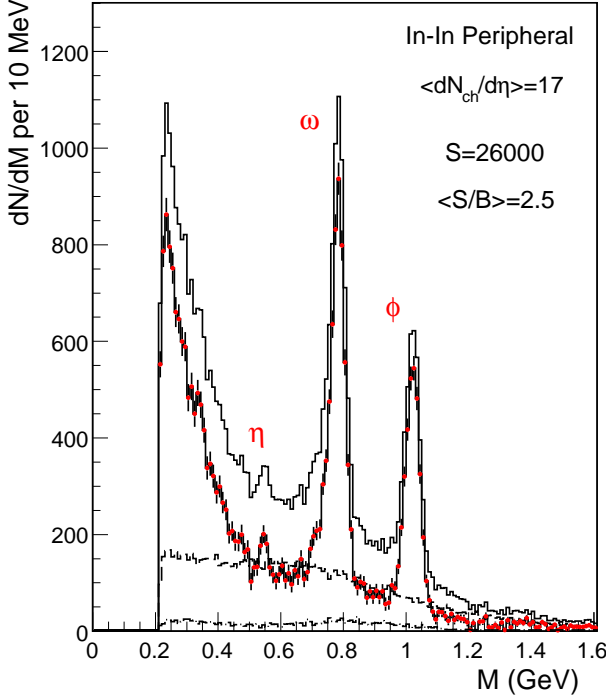


Figure 1: Mass spectra of the opposite-sign dimuons (upper histogram), combinatorial background (dashed), signal fake matches (dashed-dotted), and resulting signal (histogram with error bars).

small contributions from combinatorial background and signal fake matches, the resulting net spectrum contains about 26 000 muon pairs in the mass range 0.2-1.4 GeV. The average signal-to-background ratio is  $\sim 2.5$ . Although the relative uncertainties of the combinatorial background are  $\sim 4\%$  for the peripheral selection (larger than the 1% achieved for more central collisions [12]), the resulting systematic errors of the net data are still on the level of only about 1.5%. The vector mesons  $\omega$  and  $\phi$  are completely resolved; even the rare two-body decay  $\eta \rightarrow \mu^+\mu^-$  is seen. The mass resolution of the  $\omega$  is 20 MeV.

As shown in our previous analysis [13], the peripheral data can fully be described by the expected electromagnetic decays of the neutral mesons. In the procedure used then and updated now, muon pair production from the 2-body decays of the  $\eta$ ,  $\rho$ ,  $\omega$  and  $\phi$  resonances and the Dalitz decays of the  $\eta$ ,  $\eta'$  and  $\omega$  is simulated using the improved hadron decay generator GENESIS [14],

while GEANT is used for transport through the acceptance of the NA60 apparatus, including the effects of the dimuon trigger. The Monte Carlo data are overlaid onto real data and then reconstructed in the same way as the latter, to take account of the pair reconstruction

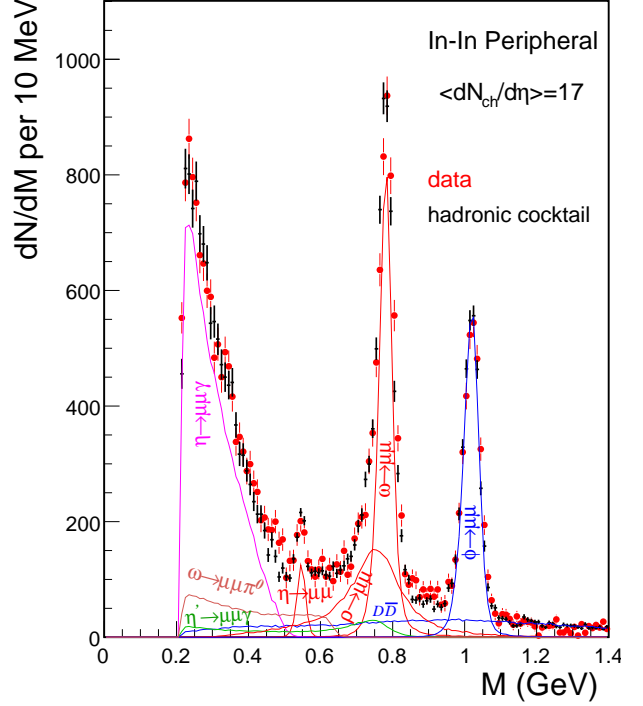


Figure 2: Signal pairs after subtraction of the total background. A superposition of the known meson decays describes the data quantitatively (see text).

efficiency. The data are fit with this “decay cocktail” of sources, using the production cross section ratios  $\eta/\omega$ ,  $\rho/\omega$ ,  $\phi/\omega$  and the level of dimuons from charm ( $D\bar{D}$ ) decays as free parameters; the ratio  $\eta'/\omega$  is kept fixed at 0.12 [14, 15]. The branching ratios of the different decays are taken from the PDG [16], and the transition form factors of the three Dalitz decays are those measured by Lepton-G [2, 5, 6] (which is also the source for the respective three branching ratios in the PDG). The  $p_T$  spectra of all hadrons ( $\eta$ ,  $\omega$ ,  $\phi$  and  $\rho$ ) entering into the acceptance filtering have been precisely measured over the full  $p_T$ -range, including their centrality dependence, and those for the peripheral selection are used here. The  $y$  distributions are also measured, confirming those in the original code [14]. The  $\cos\theta_{CS}$  distributions ( $\theta_{CS}$  is the polar angle of the muon angular distribution in the Collins-Soper reference frame) are uniform for the resonance decays as recently measured [10], and the angular distributions of the Dalitz decays are  $(1+\cos^2\theta)$  for the

$\eta$  and uniform for the  $\omega$  [14] (here  $\theta$  denotes the polar angle relative to the virtual photon direction). Data and fits, including an illustration of the individual sources, are shown in Fig. 2. The fit quality is good throughout. The only reminiscence to the excess dimuons found at the higher centralities [8, 9] is a slightly enhanced  $\rho/\omega$  ratio as compared to  $pp$  interactions [13], attributed to some contribution from  $\pi^+\pi^-$  annihilation already at  $\langle dN_{ch}/d\eta \rangle = 17$  (without in-medium effects). The form factor anomaly of the  $\omega$  Dalitz decay, responsible for the peculiar shape close to the kinematic cut-off in contrast to the  $\eta$ , is well visible in Fig. 2 and seems to be required by the data, although the description is not perfect (we will come back to that later). It is important to add that the differential acceptance variations in the full  $M$ - $p_T$  plane, including a decrease by two orders of magnitude in the region of low  $M$  and low  $p_T$  [13], have been understood to within  $\leq 10\%$  on the basis of the observed  $p_T$ -independence of the particle ratios extrapolated to full phase space [13], suggesting a significantly better accuracy in the mass domain alone.

In the subsequent analysis, we will turn the procedure around. We will isolate the Dalitz decays of the  $\eta$  and  $\omega$  as well as possible and measure the associated transition form factors without any *a priori* input to the description of the data in this region. The influence of all other decay sources on the results will be discussed in detail separately, considering the uncertainties connected to them as sources of systematic errors.

In the first step, the 2-body decays of the narrow vector mesons  $\omega$  and  $\phi$  are subtracted in the same way as done before to isolate the excess dimuons at higher centralities [8, 9]. The yields are determined such as to get, after subtraction, a *smooth* underlying continuum. As discussed previously [9], the accuracy of this procedure is very high, about 3-4% for the  $\omega$  and 2% for the  $\phi$ . These two sources are, in any case, completely outside of the mass window relevant for the study of the  $\eta$  and  $\omega$  Dalitz decays, i.e. the window  $0.2 < M < 0.65$  GeV. The sole reason for their subtraction is the isolation of the broad vector meson  $\rho$ , which is normally masked by the much narrower  $\omega$  at nearly the same mass, making it then much easier to control the systematics due to a small contribution from the low-mass tail of the  $\rho$  in the mass region of interest here. Within that region, the well resolved  $\eta \rightarrow \mu^+\mu^-$  channel, with a mass resolution of about 13 MeV, is also subtracted with high accuracy, based on the same criterion as for the  $\omega$  and  $\phi$ . The remaining sources, the  $\eta'$  Dalitz decay and charm, are only on a level of a few % each of the total yield. As will be shown in next section, the final results are completely immune to the treatment of these sources, but they will

ultimately also be taken out. After all subtractions, the remaining sample size is about 15 000 pairs,  $\sim 9$  000 for the  $\eta$  Dalitz,  $\sim 3$  000 for the  $\omega$  Dalitz and  $\sim 3$  000 for the  $\rho$ . The corresponding Lepton-G numbers for the two Dalitz decays are 600 and 60, respectively [2, 5, 6].

The treatment of the acceptance of the NA60 apparatus will also be turned around. Instead of dealing with the results after the acceptance filtering as in Figs. 1 and 2, we now *correct* the net data obtained from the first step for acceptance. The final physics outcome is, of course, invariant as to whether the analysis is done at the input or the output, i.e. before or after the acceptance filtering. The advantages of the reversal of the procedure are twofold. The large number of parameter variations in the fits to the residual data ( $> 60$ ) can much more efficiently be done at the input, without the need to propagate each choice through the complete Monte Carlo chain. In addition, the final results can then be judged on the basis of the original spectral shapes, without acceptance distortions. The acceptance is determined for the mixture of the three sources left in Fig. 3, i.e. the  $\eta$  and  $\omega$  Dalitz decays plus the  $\rho$ , using precisely the same input distributions as before and the weights as obtained from the fits to the peripheral data (Fig. 2). The resulting mass dependence is rather flat, with variations in the region of the Dalitz decays,  $0.2 < M < 0.65$  GeV, by only a factor of 2. A rise by a further factor of 2 occurs across the mass region of the  $\rho$ . For systematic studies, the relative weight of the  $\omega$ -Dalitz decay in the mixture is varied by a factor of 1.8 (for reasons to be discussed later), resulting in local changes of the acceptance by only  $\leq \pm 3\%$ .

## 4. Results

The net mass spectrum of the muon pairs after subtraction of the three narrow resonances  $\eta$ ,  $\omega$  and  $\phi$  as well as the  $\eta'$  Dalitz decay and charm (see below), corrected for acceptance and pair efficiency, is shown in Fig. 3. The ordinate is in a.u. and does not any longer reflect the measured number of counts. The spectral shape of the data in this figure looks impressive. Beyond the  $\eta$  Dalitz decay which was easily recognizable before in Figs. 1, 2 due to its dominance in the mass region  $M < 0.5$  GeV and its characteristic mass shape, the  $\rho$  now shines out completely isolated, and the  $\omega$  Dalitz decay in between becomes directly recognizable in the mass window  $0.5 < M < 0.65$  GeV through the characteristic shoulder close to the kinematic cut-off of its mass distribution. This shoulder reflects, beyond any doubt, the qualitative existence of the strong anomaly in the associated electromagnetic transition form factor [2, 6],

and the data quality in this well-isolated section raises the expectation that the extraction of the quantitative details will be possible with a high reliability. This is indeed the case.

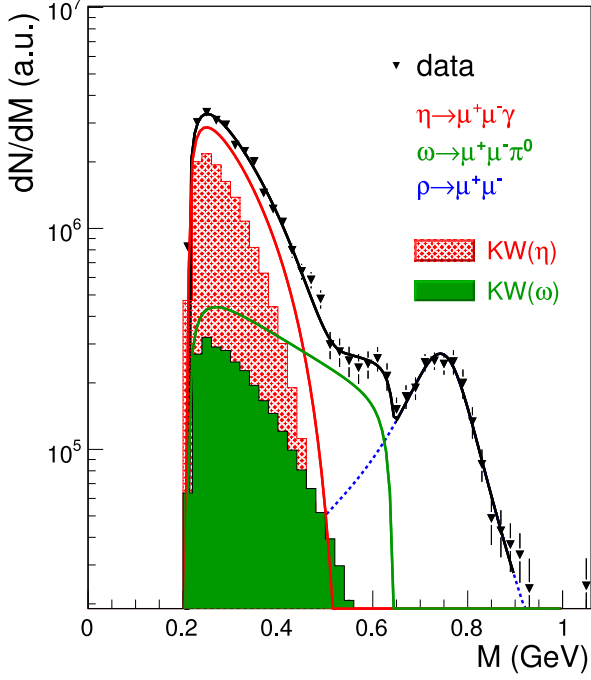


Figure 3: Acceptance-corrected mass spectrum of the muon pairs after subtraction of the  $\eta$ ,  $\omega$ ,  $\phi$  resonance decays and the nearly negligible contribution of the  $\eta'$  Dalitz decay and charm. The lines represent a fit with Eq. (5), showing the individual contributions from the  $\eta$  and  $\omega$  Dalitz decays, the  $\rho$  resonance decay and the sum of the three (see text for final fit parameters used here). The shaded areas indicate the expectations for the  $\eta$  and  $\omega$  Dalitz decays for point-like particles, defined by [QED] [1] in Eqs. (2,3).

The further study is based on global as well as local fits to the data, using a superposition of the three sources with (mostly) 5 free parameters: the yields of the three sources and the pole parameters of the form factors of the two Dalitz decays, defined already above with Eq. (1). All other physics parameters which are not strictly known will be varied to study their influence on the fits. Once the final fit parameters and their errors are fixed, the three sources in Fig. 3 will also be disentangled, making it then possible to present the form factors  $|F_i(M)|^2$  of the two Dalitz decays in the usual way.

Analytically, the dilepton mass spectrum of the Dalitz decay  $\eta \rightarrow \mu^+ \mu^- \gamma$  is given by [2, 5] ( $M = m_{\mu\mu}$ )

$$\begin{aligned} \frac{d\Gamma(\eta \rightarrow \mu^+ \mu^- \gamma)}{dm_{\mu\mu}^2} &= \frac{2}{3} \frac{\alpha}{\pi} \frac{\Gamma(\eta \rightarrow \gamma\gamma)}{m_{\mu\mu}^2} \times \left(1 - \frac{m_{\mu\mu}^2}{m_\eta^2}\right)^3 \\ &\quad \left(1 + \frac{2m_\mu^2}{m_{\mu\mu}^2}\right) \times \left(1 - \frac{4m_\mu^2}{m_{\mu\mu}^2}\right)^{1/2} \times |F_\eta(m_{\mu\mu}^2)|^2 \\ &= [\text{QED}(m_{\mu\mu}^2)] \cdot |F_\eta(m_{\mu\mu}^2)|^2, \end{aligned} \quad (2)$$

while that for the Dalitz decay  $\omega \rightarrow \mu^+ \mu^- \pi^0$  is defined by the slightly more complicated expression [2, 6]

$$\begin{aligned} \frac{d\Gamma(\omega \rightarrow \mu^+ \mu^- \pi^0)}{dm_{\mu\mu}^2} &= \frac{\alpha}{3\pi} \frac{\Gamma(\omega \rightarrow \pi^0\gamma)}{m_{\mu\mu}^2} \left(1 + \frac{2m_\mu^2}{m_{\mu\mu}^2}\right) \times \\ &\quad \left(1 - \frac{4m_\mu^2}{m_{\mu\mu}^2}\right)^{1/2} \times \left(\left(1 + \frac{m_{\mu\mu}^2}{m_\omega^2 - m_{\pi^0}^2}\right)^2 - \frac{4m_\omega^2 m_{\mu\mu}^2}{(m_\omega^2 - m_{\pi^0}^2)^2}\right)^{3/2} \\ &\quad |F_\omega(m_{\mu\mu}^2)|^2 = [\text{QED}(m_{\mu\mu}^2)] \cdot |F_\omega(m_{\mu\mu}^2)|^2 \end{aligned} \quad (3)$$

For the resonance decay  $\rho \rightarrow \mu^+ \mu^-$ , we use the line shape (including a Boltzmann term) characteristic for hadro-production of the  $\rho$  [14, 17]

$$\begin{aligned} \frac{dR_{\rho^0 \rightarrow \mu^+ \mu^-}}{dM} &= \frac{\alpha^2 m_\rho^4}{3(2\pi)^4} \frac{\left(1 - \frac{4m_\mu^2}{M^2}\right)^{3/2} \left(1 - \frac{4m_\mu^2}{M^2}\right)^{1/2} \left(1 + \frac{2m_\mu^2}{M^2}\right)}{(M^2 - m_\rho^2)^2 + M^2 \Gamma_{\text{tot}}^2} \\ &\quad \times (2\pi M T)^{3/2} e^{-\frac{M}{T}} \end{aligned} \quad (4)$$

The fit function with the 5 free parameters  $A_i$  and  $\Lambda_i^{-2}$  can then be written in the form

$$\frac{dN}{dM} = A_\eta f_\eta(M, \Lambda_\eta^{-2}) + A_\omega f_\omega(M, \Lambda_\omega^{-2}) + A_\rho f_\rho(M) \quad (5)$$

where the mass differential functions  $f_i$  contain the full information of Eqs. (2–4).

The specific fit shown in Fig. 3 illustrates already the final outcome: the individual fit lines for the two Dalitz decays are above the respective QED expectation, implying the form factors to be consistently  $>1$  and actually  $\gg 1$  for the  $\omega$  spectrum close to its kinematic limit.

The interest in leaving the yields of the Dalitz decays also free in the fits is connected to their branching ratios. As a byproduct to the form factor studies, these can directly be measured by relating the yields to those of the respective resonance decays, which are subtracted but known. In case of the  $\eta$ , the experimental error of the decay  $\eta \rightarrow \mu^+ \mu^-$  is unfortunately  $\sim 30\%$ , much larger than those of either of the two branching ratios [16]; there is thus no chance for improvements. In case of the  $\omega$ , however, the errors of the reference

decay  $\omega \rightarrow \mu^+\mu^-$  are quite small: 3-4% for the measured yield in Fig. 2 and 2% for the branching ratio, if we replace the  $\mu^+\mu^-$  value  $(9.0\pm 3.1)\cdot 10^{-5}$  by the much more accurate  $e^+e^-$  value  $(7.16\pm 0.12)\cdot 10^{-5}$  [16] as justified by lepton universality. In contrast, the error of the branching ratio of the Dalitz decay  $\text{BR}(\omega \rightarrow \mu^+\mu^-\pi^0) = (9.6\pm 2.3)\cdot 10^{-5}$  [6, 16] is much larger, 24%, opening a realistic chance for a more accurate measurement of the latter. The outcome will indeed be a larger value, and the two acceptance options mentioned before take care of this initial ambiguity in the mixture of sources, labeled in the following *A* (for the new value) and *B* (for the PDG value).

Altogether, about 60 different fits were done, varying a number of parameters and their combinations. The parameters were the following. The acceptance had the options *A* and *B*. The temperature parameter  $T_\rho$  of the  $\rho$ , so far unmeasured in  $pp$ -like interactions, had the options 170 and 140 MeV, while the pole mass and width of the  $\rho$  were (mostly) fixed at  $M_\rho = 0.770$  and  $\Gamma_\rho = 0.150$  GeV [16], respectively. Since the acceptance-corrected data still contain the resolution smearing of the NA60 set-up, resolution smearing was imposed on the fit function Eq. (5) to study the sensitivity. The contribution of the  $\eta'$  Dalitz decay was either fully left in the data sample, or subtracted under the different assumptions  $\eta'/\omega=0.12$  [14, 15], 0.24, 0.36 or 0.48, amounting to subtracted fractions of only 1%, 2%, 3% and 4% of the full yield in the mass region  $M<0.64$  GeV. The contribution from charm ( $D\bar{D}$  decays) was either fully left in the data sample, or subtracted under the different assumptions of 30%, 60% or 100% of the total yield in the mass window  $1.2<M<1.4$  GeV to be charm (and Drell-Yan), amounting to subtracted fractions of 1%, 2% and 4% of the total yield in the mass region  $M<0.64$  GeV. Specific fits were done (i) with a branching ratio of the  $\omega$  Dalitz decay frozen to the PDG value, and (ii) with the temperature parameter  $T_\rho$  of the  $\rho$  also left as a free parameter. Fit ranges were mostly global, covering the complete mass range  $0.2<M<0.9$  GeV, but for specific goals also local, like  $0.5<M<0.9$  GeV. The quality of the fits for each parameter combination was judged by the respective  $\chi^2/ndf$ , assessed globally in the complete mass range  $0.2<M<0.9$  GeV, but also locally in the subwindows  $0.2<M<0.48$  GeV ( $\sim 80\%$   $\eta$  Dalitz),  $0.48<M<0.66$  ( $\sim 67\%$   $\omega$  Dalitz),  $0.66<M<0.86$  ( $\sim 100\%$   $\rho$ ), and  $0.75<M<0.95$  GeV (upper tail of the  $\rho$ ). The detailed results from the individual 60 fits, including the values of the fit quantities, their errors, the  $\chi^2/ndf$  in the individual windows and a number of further aspects of the analysis can be found in a publicly accessible NA60 Internal Note [18]. Here, we restrict

ourselves to a summary of the results and the associated systematics.

Very generally, the fits have been found to give remarkably stable and reproducible results. The fit quality in the mass region of the two Dalitz decays, i.e.  $M<0.65$  GeV, is completely insensitive to variations of the acceptance, of  $T_\rho$ , of the resolution folding, and of the fraction of subtraction of the  $\eta'$  and charm contributions. The values of  $\chi^2/ndf$  are always  $\sim 1$ , and the variations of the extracted fit parameters are mostly  $<1/2$  of the (statistical) fit errors. Given this situation, we quote the final values of the fit parameters as the (unweighted) average over all measured values, their statistical errors as the average over the fit errors (which hardly vary at all), and their systematic errors as the *rms* deviation of the individual values from the average. The ratio systematic/statistical errors is about 0.3 for the two pole parameters, and about 0.5 for the  $\omega$ -Dalitz branching ratio.

However, the mass region outside of interest here, i.e.  $M>0.65$  GeV and in particular the high-mass tail of the  $\rho$ , is indeed sensitive to the variations of some of the parameters, and the extracted values of  $\chi^2/ndf$  can reach up to values of 7. The global conclusions from this part of the analysis are a clear preference for the higher temperature of the  $\rho$ , for a subtraction of the  $\eta'$  Dalitz contribution on the level of at most  $\eta'/\omega=0.12$  [14, 15], and for a full subtraction of the charm contribution. It is for this reason and *not* for reasons of any sensitivity in the region of the  $\eta$  and  $\omega$  Dalitz decays, that these specific  $\eta'$  and charm contributions have been subtracted for the data sample selected for Fig. 3.

A final comment on systematics. The analysis procedure as used is self-consistent: the acceptance has been assessed on the basis of measured data throughout, including the anomalous form factor of the  $\omega$ . However, the results are extremely robust as to deviations from that. For the  $\omega$ , e.g., usage of the VMD form factor in the simulations leads to drastic deficits in the description of the (acceptance-filtered) data in Fig. 2 [18]. Yet, an acceptance correction based on such an inferior description, with quite different (mass-dependent) weights of the 3 sources to before, still leaves the characteristic shoulder of the  $\omega$  Dalitz decay (Fig. 3) essentially unchanged, and the fit value of the pole parameter is found to only change by about 1 standard deviation (statistical) [18]. It hardly needs to be stressed that the self-consistent results obtained from fits at the input, i.e. after acceptance correction, are found to be absolutely identical to those obtained from fits to the directly measured data, i.e. before acceptance correction [18].

In detail, the following numerical results have been obtained.

The pole parameter of the electromagnetic transition form factor of the Dalitz decay  $\eta \rightarrow \mu^+ \mu^- \gamma$  is measured to be  $\Lambda_\eta^{-2} = 1.95 \pm 0.17(\text{stat.}) \pm 0.05(\text{syst.}) \text{ GeV}^{-2}$ . It perfectly agrees with the previous measurement of the Lepton-G experiment  $\Lambda_\eta^{-2} = 1.90 \pm 0.40 \text{ GeV}^{-2}$  as well as with predictions from VMD,  $\Lambda_\eta^{-2} = 1.8$

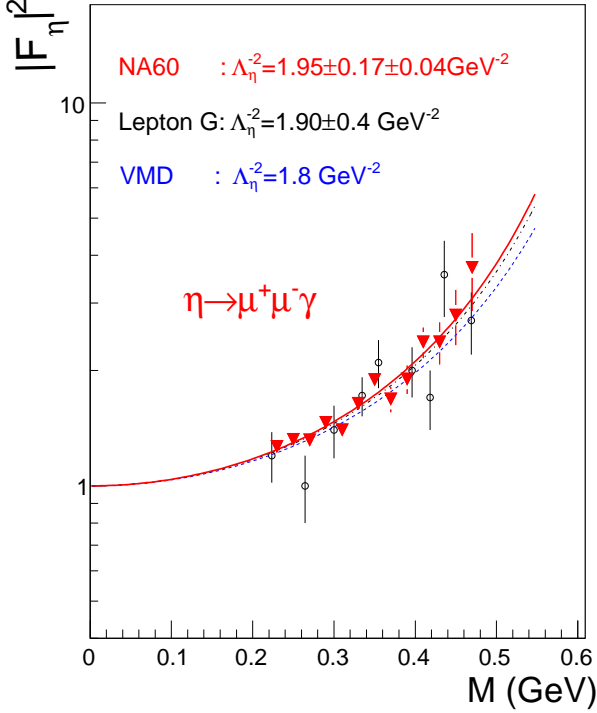


Figure 4: Experimental data on the  $\eta$ -meson electromagnetic transition form factor (red triangles), compared to the previous measurement by the Lepton-G experiment (open circles) and to the expectation from VMD (blue dashed line). The solid red and black dashed-dotted lines are results of fitting the experimental data with the pole dependence Eq. (1). The normalization is such that  $|F_\eta(M=0)|=1$ .

$\text{GeV}^{-2}$  [2]. The characteristic mass  $\Lambda$  is equal to  $\Lambda_\eta = 0.716 \pm 0.031(\text{stat.}) \pm 0.009(\text{syst.}) \text{ GeV}$ , as compared to the value from Lepton-G of  $\Lambda_\eta = 0.724 \pm 0.076 \text{ GeV}$  or to the VMD value of  $\Lambda_\eta = 0.745 \text{ GeV}$ . Our result improves the Lepton-G error by a factor of 2.3, equivalent to a factor of 5 larger statistics. The error improvement to be expected from the difference in sample sizes (9 000 vs. 600) would have been larger (a factor of 3.8), but this is only found if the  $\omega$  Dalitz decay is frozen in the fit [18].

The pole parameter of the electromagnetic transition form factor of the Dalitz decay  $\omega \rightarrow \mu^+ \mu^- \pi^0$  is measured to be  $\Lambda_\omega^{-2} = 2.24 \pm 0.06(\text{stat.}) \pm 0.02(\text{syst.}) \text{ GeV}^{-2}$ . Within errors, it agrees with the Lepton-G value of  $\Lambda_\omega^{-2} = 2.36 \pm 0.21 \text{ GeV}^{-2}$ . Both experimen-

tal results differ from the expectation of VMD of  $\Lambda_\omega^{-2} = 1.68 \text{ GeV}^{-2}$  [2]. The *anomaly* is therefore fully confirmed. The characteristic mass  $\Lambda$  is found to be  $\Lambda_\omega = 0.668 \pm 0.009(\text{stat.}) \pm 0.003(\text{syst.}) \text{ GeV}$ , as compared to the value from Lepton-G of  $\Lambda_\omega = 0.65 \pm 0.03 \text{ GeV}$  or to the VMD value of  $\Lambda_\omega = M_\rho = 0.770 \text{ GeV}$ . The confirma-

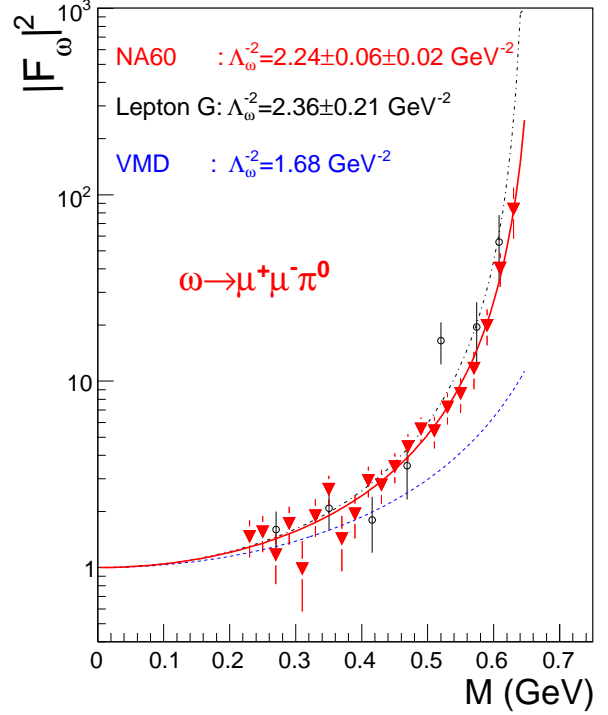


Figure 5: Experimental data on the  $\omega$ -meson electromagnetic transition form factor (red triangles), compared to the previous measurement by the Lepton-G experiment (open circles) and to the expectation from VMD (blue dashed line). The solid red and black dashed-dotted lines are results of fitting the experimental data with the pole dependence Eq. (1). The normalization is such that  $|F_\omega(M=0)|=1$ .

tion of the anomaly receives particular weight through the fact that the statistical errors are improved by a factor of nearly 4, equivalent to a statistics larger by a factor of  $>10$ . Referred to  $\Lambda^{-2}$ , the previous measurement differed by three standard deviations ( $3\sigma$ ) from the VMD expectation, while our new measurement differs by  $10\sigma$ . The error improvement to be expected from the difference in sample sizes (3 000 vs. 60) would have been still larger (by a factor of 7), but this is only found if the  $\eta$  Dalitz decay is frozen in the fit [18].

The branching ratio of the  $\omega$  Dalitz decay  $\text{BR}(\omega \rightarrow \mu^+ \mu^- \pi^0)$  is found to be larger by a factor of  $1.79 \pm 0.26(\text{stat.}) \pm 0.15(\text{syst.})$  than that of the PDG [16], i.e. Lepton-G [6], corresponding to a new absolute value of  $(1.72 \pm 0.25(\text{stat.}) \pm 0.14(\text{syst.})) \cdot 10^{-4}$ . Taking ac-

count also of the 24% error of the PDG value, the two values of the branching ratio differ by 2 standard deviations, hardly significant. It is interesting to note that there is no contradiction between the increased branching ratio as obtained from the present systematic fits and the previous description of the data on the basis of the PDG value as shown in Fig. 2. On the contrary, a deficit of the sum of the generated events in the mass region  $0.48 < M < 0.64$  GeV compared to the data (subtracting the  $\eta \rightarrow \mu^+\mu^-$  channel also there) clearly exists, reflected by a  $\chi^2/ndf$  of about 5 in that region of Fig. 2. For  $M > 0.55$  GeV, this is partially compensated for by the effects of the higher pole parameter value from Lepton-G. Specific fits done to scrutinize such a compensation fail for the present data, however, thanks to the much higher data quality. Fixing the branching ratio to the PDG value and varying the pole parameter, the description of the data is already visually unacceptable for any choice of the pole parameter, and the minimal value of  $\chi^2/ndf$  reached is about 3.3 [18].

From a series of specific fits, leaving the temperature parameter  $T_\rho$  in the line-shape description of the  $\rho$  also free, the average value of  $T_\rho$  is found to be  $170 \pm 19(\text{stat.}) \pm 3(\text{syst.})$  MeV. Since the event selection is peripheral In-In, with  $\langle dN_{ch}/d\eta \rangle \sim 17$ , there will hardly be an in-medium influence on the value. We interpret this number to reflect the effective temperature of the system at the time of creation, making it consistent with the same value of 170 MeV obtained by statistical model fits of particle ratios in  $pp$  interactions. This is the first time in the literature that  $T_\rho$  has been determined experimentally.

The specific simulation lines shown in Fig. 3 are actually based on the average fit parameters discussed in the preceding four paragraphs. Starting from here, we finally present the results on the transition form factors in the traditional way. In a first step, we isolate the individual Dalitz contributions in the spectrum of Fig. 3, subtracting the contribution of the  $\rho \rightarrow \mu^+\mu^-$  decay and disentangling the  $\eta \rightarrow \mu^+\mu^-\gamma$  and  $\omega \rightarrow \mu^+\mu^-\pi^0$  decays as determined by the fits. This implies to use the same individual data points for the  $\eta$  and the  $\omega$ , subtracting for the  $\eta$  the fit results of the  $\omega$  and vice versa. With  $|F_i(M)|^2 \rightarrow 1$  for  $M \rightarrow 0$ , the individual normalizations are automatically fixed, and the QED and the form factor parts can be separately assessed. In a second step, the squared form factors  $|F_i(M)|^2$  are obtained by dividing the difference data for the respective decay by its QED part.

The results for the  $\eta$  and the  $\omega$  are plotted in Figs. 4 and 5, respectively, keeping the data-point errors from Fig. 3. The pole parameters and their errors as obtained

from the combined fits to both Dalitz decays are shown as inserts. Note that these are the correct values, while independent fits through the data points of Figs. 4 and 5 would automatically result in somewhat smaller errors of the pole parameters, since the respective other decay appears as fixed. The errors shown are statistical errors. The systematic errors are smaller than the statistical ones as outlined above. For the  $\omega$  form factor in the mass region  $< 0.45$  GeV, where the  $\eta$  Dalitz decay dominates in the total mass spectrum (see Fig. 3), this has explicitly been verified (on top of all other sources) by varying the form factors of the two Dalitz decays in the global fit procedure preceding the isolation [18]. Both figures also include the Lepton-G data [2, 5, 6] and the expectations from VMD [2, 5, 6] for comparison. Within the large errors of the Lepton-G data, perfect agreement between the two data sets is seen in both cases, while the great improvement in data quality of the present results is completely apparent. Irrespective of the much reduced errors, the form factor of the  $\eta$  is still close to the expectations from VMD. The form factor of the  $\omega$ , on the other hand, strongly deviates from VMD, showing a further (relative) increase close to the kinematic cut-off by a factor of  $\sim 10$ , and a factor of altogether  $\sim 100$  relative to the pure QED part.

Theoretically, the most elementary description of the transition form factors in terms of VMD does not only work reasonably well for the Dalitz decay of the  $\eta$ , but also for that of the  $\eta'$ , at least within the very large errors there [2]. The anomaly of the  $\omega$  case has been a puzzle from the beginning. Slight enhancements of the  $\omega$  form factor beyond VMD have been obtained historically on the basis of a modified  $\rho$  propagator [19] and a nonlocal quark model [20]. More recent calculations on the basis of an effective Lagrangian approach to vector mesons [21], and of an extended VMD model including up to two excited  $\rho$  states [22], do somewhat better, but now overestimate the form factor at low  $M$  and still underestimate it at high  $M$  in the region of the kinematic cut-off. One might rightly expect that our improved data will initiate new theoretical efforts to finally understand the physics behind.

## 5. Conclusions

To summarize, we have been able to measure the electromagnetic transition form factors of the  $\eta$  and  $\omega$  Dalitz decays with a much better precision than reached before, confirming after nearly 30 years the strong anomaly associated with the  $\omega$ . A satisfactory theoretical understanding is still pending. On purely empirical



grounds, the new results will greatly diminish the uncertainties of direct dilepton measurements in this particular mass region. As a byproduct, we have also obtained an improved value for the branching ratio of the  $\omega$  Dalitz decay.

## Acknowledgments

We acknowledge support from the BMBF (Heidelberg group) as well as from the C. Gulbenkian Foundation and the Swiss Fund Kidagan (YerPHI group).

## References

- [1] N. M. Kroll and W. Wada, *Phys. Rev.* **98** (1955) 1355
- [2] L. G. Landsberg *et al.*, *Phys. Reports* **128** (1985) 301
- [3] M. N. Achasov *et al.*, *Phys. Lett. B* **504** (2001) 275
- [4] R. R. Akhmetshin *et al.*, *Phys. Lett. B* **613** (2005) 29
- [5] R. I. Djeliadin *et al.*, *Phys. Lett. B* **94** (1980) 548
- [6] R. I. Djeliadin *et al.*, *Phys. Lett. B* **102** (1981) 296
- [7] G. Agakichiev *et al.* (CERES Collaboration), *Eur. Phys. J. C* **41** (2005) 475; arXiv:nucl-ex/0506002
- [8] R. Arnaldi *et al.* (NA60 Collaboration), *Phys. Rev. Lett.* **96**, 162302 (2006); arXiv:nucl-ex/0605007
- [9] R. Arnaldi *et al.* (NA60 Collaboration), *Phys. Rev. Lett.* **100**, 022302 (2008); arXiv:0711.1816 [nucl-ex]
- [10] R. Arnaldi *et al.* (NA60 Collaboration), Submitted to *Phys. Rev. Lett.* (2008); arXiv:0812.3100 [nucl-ex]
- [11] D. Adamova *et al.* (CERES Collaboration), *Phys. Lett. B* **666** (2008) 425
- [12] R. Shahoyan *et al.* (NA60 Collaboration), in press, *Eur. Phys. J.* (2008); arXiv:0810.3204
- [13] S. Damjanovic *et al.* (NA60 Collaboration), *Eur. Phys. J. C* **49** (2007) 235; arXiv:nucl-ex/0609026
- [14] S. Damjanovic, A. De Falco and H. Wöhri, NA60 Internal Note 2005-1
- [15] F. Becattini *et al.*, *Phys. Rev. C* **69** (2004) 024905
- [16] C. Amsler *et al.* (Particle Data Group), *Phys. Lett. B* **667** (2008) 1
- [17] R. Rapp, J. Wambach and H. van Hees, (2009) arXiv:0901.3289 [hep-ph]
- [18] S. Damjanovic and H. J. Specht, NA60 Internal Note 2009-1
- [19] G. Kopp, *Phys. Rev. D* **10** (1974) 932
- [20] G. V. Efimov *et al.*, *Pisma Z. Eksp. Teor. Fiz.* 32 (1980) 1; 60; M. Dinejhan *et al.*, *Proc. Yad. Fiz.* 34 (1981) 264
- [21] F. Klingl, N. Kaiser and W. Weise, *Z. Phys. A* **356** (1996) 193
- [22] A. Faessler, C. Fuchs and M. I. Krivoruchenko, *Phys. Rev. C* **61** (2000) 035206; private communication (2009)